

## Variable stars detection in the field of open cluster NGC 188

Fang-Fang Song<sup>1,2</sup>, Hu-Biao Niu<sup>1,2</sup>, Ali Esamdin<sup>1,2</sup>, Yu Zhang<sup>1,2</sup> and Xiang-Yun Zeng<sup>3</sup>

<sup>1</sup> Xinjiang Astronomical Observatory, Chinese Academy of Sciences, Urumqi, Xinjiang 830011, People's Republic of China; [niuhubiao@xao.ac.cn](mailto:niuhubiao@xao.ac.cn)

<sup>2</sup> School of Astronomy and Space Science, University of Chinese Academy of Sciences, Beijing 100049, People's Republic of China;

<sup>3</sup> Center for Astronomy and Space Sciences, China Three Gorges University, Yichang 443000, People's Republic of China.

Received 20xx month day; accepted 20xx month day

**Abstract** This work presents the charge-coupled device (CCD) photometric survey of the old open cluster NGC 188. Time-series V-band photometric observations were conducted for ten nights in January 2017 using the Nanshan One-meter Wide-field Telescope (NOWT) to search for variable stars in the field of the cluster field. A total of 25 variable stars, including one new variable star, were detected in the target field. Among the detected variables, 16 are cluster member stars, and the others are identified as field stars. The periods, radial velocities, effective temperatures, and classifications of the detected variables are discussed in this work. Most of the stars' effective temperatures are between 4200 K and 6600 K, indicating their spectral types are G or K. The newly discovered variable is probably a W UMa system. In this study, a known cluster variable star (V21 = V0769 Cep) is classified as an EA-type variable star based on the presence of an 0.5 magnitude eclipse in its light curve.

**Key words:** Galaxy — open cluster: individual: NGC 188 — stars: variables: general — technique: photometric — method: data analysis

### 1 INTRODUCTION

Open Clusters (OCs), which are composed of young stars, are crucial for studying the formation and evolution of the stellars and Galactic disk (Piskunov et al. 2006; Özeren et al. 2014; Gillen et al. 2020). Because the cluster members born from the same interstellar cloud are assumed to have a common age, distance, reddening, and chemical abundance, the studies in cluster variables provide significant clues to probe the structure and evolution of stars and clusters. The high precision in the astrometric and photometric measurements by Gaia gives more opportunities to classify the cluster member stars from the field stars, which is great progress for the studies of variable stars in the open clusters (Gaia Collaboration et al. 2016; Cantat-Gaudin et al. 2020).

As one of the most ancient, rich open clusters known in our Milky Way, NGC 188 ( $l = 122.843$  deg,  $b = +22.384$  deg; C 0039+850) is a captivating open cluster that is intensively studied by numerous studies (Sarajedini et al. 1999; Friel, Jacobson, & Pilachowski 2010; Hills et al. 2015; Cohen, Geller, & von Hippel 2020). It is an excellent laboratory based on its abundant member stars, easy to observe, and less contaminated by field stars owing to its special location that it is Located at high latitude and far away from the galactic disk (Bonatto, Bica, & Santos 2005; Fornal et al. 2007; Wang et al. 2015). 857 cluster member stars with probabilities over 70% was identified by Cantat-Gaudin et al. (2020).

Lists of the previous observational surveys for the cluster are shown in Fornal et al. (2007); Geller et al. (2008); Wang et al. (2015). Various works about the fundamental parameters of NGC 188 have been performed after the release of the Gaia data which provide the unprecedented precise parallax measurements (Cantat-Gaudin et al. 2020; Monteiro et al. 2020; Bonatto 2019; Gaia Collaboration et al. 2018). Taken the fitted parameters by Cantat-Gaudin et al. (2020), The basic cluster parameters of NGC 188 are as follows, the distance modulus 11.15 mag, corresponding to the distance 1698 pc,  $\log(\text{Age}) = 9.85\text{yr}$ , extinction  $A_V = 0.21\text{mag}$ .

Also, NGC 188 is a special cluster owing for its abundant and various variable stars. Early in the 1960s, four short-period W UMa stars (known as EQ Cep, ER Cep, ES Cep, EP Cep) and a suspected variable NSV 395 were discovered by Hoffmeister (1964). Kaluzny & Shara (1987) and Kaluzny (1990) discovered another 7 short-period variables through CCD photometric surveys using the 0.9 m telescope at Kitt Peak National Observatory (KPNO). Subsequently, Xin, Zhang, & Deng (2002) and Zhang et al. (2004) yielded sixteen variables by monitoring the cluster in  $1 \text{ deg}^2$  field with the 60/90-cm Schmidt telescope located at the Xinglong Station of the National Astronomical Observatories of the Chinese Academy of Sciences. Meanwhile, Kafka & Honeycutt (2003) reported 51 faint variables in the cluster's central area of  $17 \times 17 \text{ arcmin}^2$  with the WIYN 3.5-m telescope, but only two variables were detected by the subsequent monitoring of other telescopes. Another 18 variables were discovered by Mochejska et al. (2008) as the results of searching for transiting planets in the open cluster NGC 188, part of the project of Planets in Stellar Clusters Extensive Search (PISCES). In the field of  $1.5 \times 1.5 \text{ deg}^2$  around the cluster, 18 new variable stars were identified by the MASTER series robotic telescope in the Astronomical Observatory of Ural Federal University (Popov et al. 2013). These variable stars were included in the electronic catalog of the American Association of Variable Star Observers (AAVSO/VSX<sup>1</sup>) in which 68 variable stars are known within a 30 arcmin radius around NGC 188. The Gaia collaboration identified another 61 variable stars based on the the Gaia DR3 database (Gaia Collaboration 2022). A total of 129 variables were collected in this field.

This paper is structured as follows. In Section 2 the observations and data reductions are presented. We focused on the variable identification and memberships in Section 3. In Section 4 we compared our results with previous works and emphasized our work of the new variable star. The conclusions are given in Section 5.

## 2 OBSERVATIONS AND DATA REDUCTIONS

In January 2017, ten days of photometric observations were conducted by using the Nanshan One-meter Wide-field Telescope (NOWT; Song et al. (2016); Ma et al. (2018); Bai et al. (2020)) located at the Nanshan station of Xinjiang Astronomical Observatory (XAO), Chinese Academy of Sciences (CAS). An E2V CCD203-82 (blue) chip CCD camera with  $4096 \times 4136$  pixels was mounted at the prime focus of the telescope, providing a field of view (FOV) of  $1.3 \times 1.3 \text{ deg}^2$ . The telescope was equipped with a Johnson-Cousins standard UBVIR filter system for broadband photometry and operated at  $-120^\circ\text{C}$  with liquid nitrogen cooling. During the observations, a number of bias and twilight flat frames were taken, and the seeing in all of these images was below 2.2 arcsec. In total, over 79 hours with 4198 images of useful data were obtained on 10 nights. The journal of the observations of NGC 188 is listed in Table 1. The exposure time of time-series observations for the V band is 35s. And the typical field of view in this period is  $54.62 \times 45.2 \text{ arcmin}^2$ , corresponding to  $2900 \times 2400$  pixels. The observed field of NGC 188 is shown in Figure 1.

The data reduction steps followed the standard procedures employed for optical CCD aperture photometry. The observed images were pre-processed by IRAF<sup>2</sup> for overscan and bias subtraction and division flat-fields correction. The dark correction was ignored because the telescope was operated in a low-temperature environment and the thermionic noise was less than  $1 \text{ e pix}^{-1} \text{ h}^{-1}$ . The instrumental magnitudes of the stars in each frame were extracted by the automated photometric software

<sup>1</sup> <http://www.aavso.org/vsx/>

<sup>2</sup> Image Reduction and Analysis Facility, <http://iraf.noao.edu/>

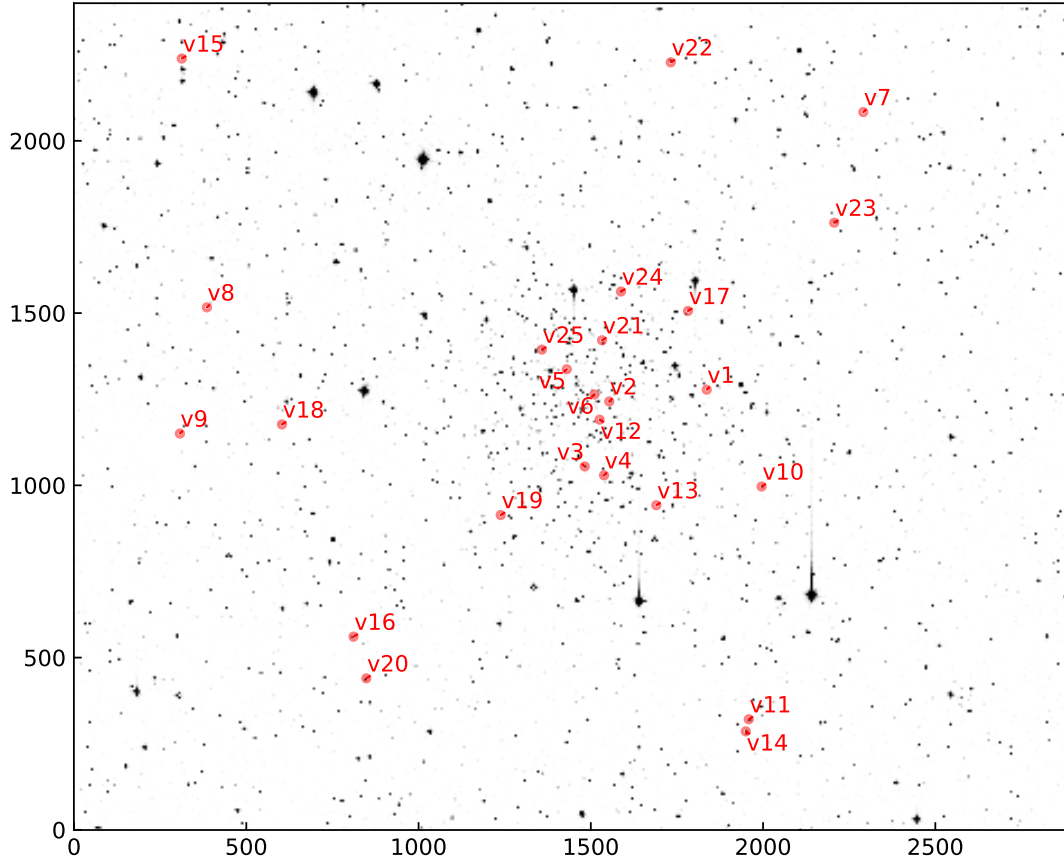


Fig. 1: The field of NGC 188 observed using the Nanshan One-meter Wide-field Telescope (NOWT) with the detected variable stars marked in red circles. North is up and east is to the left.

Table 1: Journal of CCD photometric observations for NGC 188 where N represents the number of images and Exp represents observation exposure time for each filter.

UT date	Object	Pixel	Duration (Hour)	V (N×Exp)
05 Jan 2017	NGC 188	2900×2400	1.2	38 × 35s
06 Jan 2017	NGC 188	2900×2400	1.8	58 × 35s
07 Jan 2017	NGC 188	4096×4136	5.1	171 × 35s
		2900×2400	2.6	110 × 35s
08 Jan 2017	NGC 188	2600×2400	4.5	267 × 35s
		2900×2400	5.4	290 × 35s
09 Jan 2017	NGC 188	2900×2400	12.5	649 × 35s
10 Jan 2017	NGC 188	2900×2400	12.5	657 × 35s
11 Jan 2017	NGC 188	2900×2400	11.0	598 × 35s
12 Jan 2017	NGC 188	2900×2400	0.7	67 × 35s
13 Jan 2017	NGC 188	2900×2400	9.7	502 × 35s
14 Jan 2017	NGC 188	2900×2400	12.5	666 × 35s

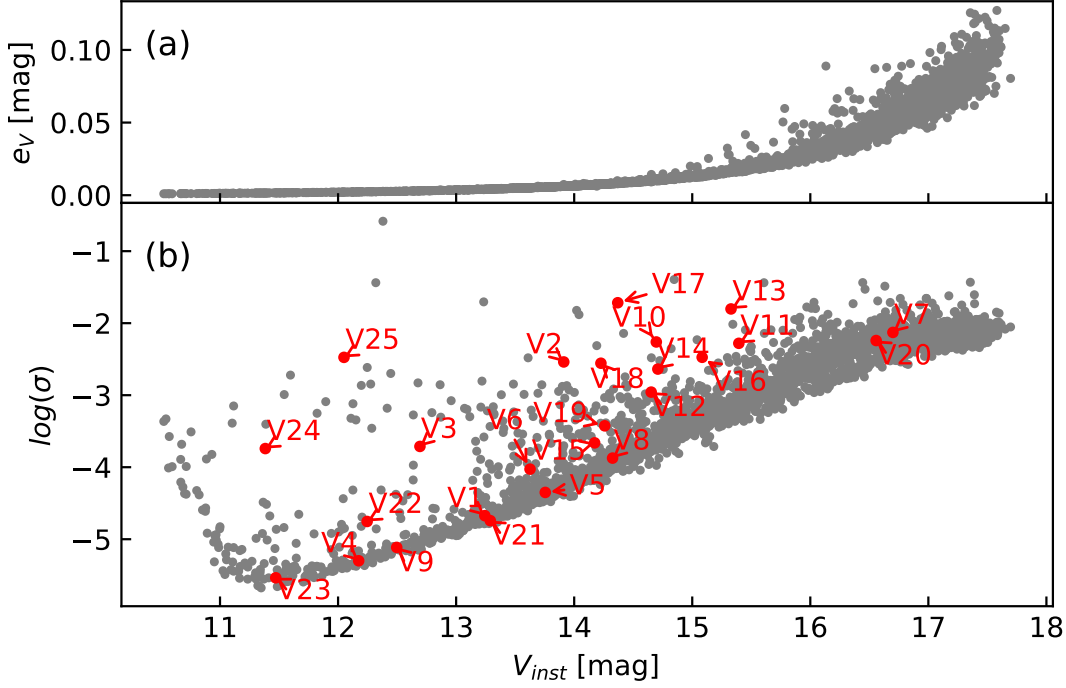


Fig. 2: Panel(a) represents the photometric errors of this work as a function of instrumental magnitude in the V band, meanwhile, Panel(b) is the standard deviation as a function of magnitude. The red dots represent the variables stars identified in this work.

SExtractor(Bertin & Arnouts 1996) and the equatorial coordinates (RA, DEC) for each detected star were computed by triangular matching with the UCAC4 (Zacharias et al. 2013). Figure 2 (a) represents the photometric errors of this work as a function of instrumental magnitudes in the V band, which indicates that the photometric errors are less than 0.1 mag when the observational magnitudes are brighter than 17 mag. Following the same procedure described in Song et al. (2016); Ma et al. (2018); Li et al. (2021), the differential light curves of 3585 stars were obtained using the data processing system of our XAO time-domain survey pipeline.

### 3 VARIABLES IDENTIFICATION

We examined the light curves of all detected stars by visual inspection and found 25 stars with obvious light variability. These variables were carefully examined for any blending or contaminating by neighboring stars. The main characteristics of the 25 variable stars are given in Table 2. The finding chart of these variable stars in the field of the cluster are shown in Figure 1. These stars are not at the edge of CCD frames, and their light curves do not have outliers. The light variations of these variables can be seen in Figures 3 and 4. To investigate the spread in data points for variable stars, Figure 2 (b) demonstrates the root-mean-square (RMS, labeled as  $\sigma$ ) scatter as a function of instrumental V magnitude. It indicates that, in general, detected variable stars (the red dots) have larger standard deviation in magnitude compared to non-variable stars.

The periods of periodic variable stars were obtained by the Generalized Lomb-Scargle Periodogram (GLS; Zechmeister & Kürster (2009)) considering the effect of noise as a sub-package of PyAstronomy (Czesla et al. 2019). The generalised Lomb-Scargle periodogram computes the error-weighted Lomb-Scargle periodogram, and provides more accurate frequencies compared with the Lomb-Scargle peri-

odogram. The adopted periods correspond to the frequency of the maximum power and the accuracies of those values are influenced by the mean magnitude, amplitude, and measurement errors. To avoid false variability arising solely due to the aliasing effect, we rechecked all the calculated periods and none of them can be seen as a factor of one day. After binning in intervals of 0.01 phase, we calculate the mean magnitude in each bin. The resulting phase-folded light curves of periodic variables are shown in Figures 3. Our data are insufficient to yield accurate periods for the other 7 long-period variable stars, and the light curves of these variables are shown in Figure 4.

For the amplitudes of the periodic variables, phased data were sorted from small to large first, then we averaged the sorted data with a sampling interval of 60 data points using the moving average method (Shan et al. 2022). Then the amplitude of the variation in periodic variables was calculated by subtracting the minimum values from the maximum values. We did almost the same operation for the amplitudes of other detected variables, except that the data were sorted by Julian Dates. Bai et al. (2019) gives the stellar effective temperature regression for the second Gaia data release applied the supervised machine-learning algorithm, based on the combination of the stars in four spectroscopic surveys: the Large Sky Area Multi-Object Fiber Spectroscopic Telescope, Sloan Extension for Galactic Understanding and Exploration, the Apache Point Observatory Galactic Evolution Experiment, and the Radial Velocity Extension. We have given the effective temperatures of most variables by cross-match the coordinates with Bai et al. (2019), except V11 and V15, which have no values of effective temperatures given in this table due to inconformity with source selection criteria of Bai et al. (2019). The effective temperature of these variable stars ranges from 4200 to 6700K, corresponding to the spectral types of K - F types.

The identified variables were cross-checked with the International Variable Star Index (VSX<sup>3</sup>) and the catalogue of Gaia DR3 Part 4 Variability (Gaia Collaboration 2022), and found most variables are matched with the online catalogs except one star V18, which implies that in our sample only V18 is a new discovery. The periods, amplitudes and shapes of the light curves of known stars produced by this work are mostly consistent with those given on the VSX website. We found an about 0.5 mag eclipse appeared in the light curve of V21, which implies that it could be an Algol-type eclipsing binary rather than a BY Draconis-type variable star given by Mochejska et al. (2008).

### 3.1 Cluster membership of the detected variables

To identify the cluster membership of the detected variable stars in this work, we cross-matched our coordinates of variable stars with Cantat-Gaudin et al. (2020), for which provided 857 cluster members with probabilities over 70% of open cluster NGC 188 using the membership assignment code Unsupervised Photometric Membership Assignment in Stellar Clusters (UPMASK, Krone-Martins & Moitinho (2014)) based on the Gaia DR2 database (Evans et al. 2018). Fourteen variables are identified as cluster members with 100% membership probabilities and the others are possible field stars for their larger proper motions in declination direction compared with cluster members.

Tarricq et al. (2022) points out that Cantat-Gaudin et al. (2018) might ignore the cluster members in the peripheral regions of OCs. In order not to miss the cluster member variables, we took advantage of Gaia DR3 (Gaia Collaboration 2022), which provides more exquisite astrometric precision than Gaia DR2, to revisit the memberships of the detected variable stars. First, we queried a cone of 30 arcmin radius around the cluster centre with non-zero astrometric and photometric parameters, as well as errors in G mag smaller than 0.005, to create Basic Sources. Figure 5 (a) presents the spatial positions of the Basic Sources and the 25 variable stars. The Basic Sources and variables are represented in grey and red/blue dots. The cluster members are obviously concentrated in the space center. In proper motion space, as shown in Figure 5 (b), we set a blue circular region centered on  $(pmRA, pmDE) = (-2.307, -0.960) mas/yr$  with radius  $1.0 mas/yr$  as the selection criteria, and fifteen variable stars are contained in the circle which are labeled in red dots, including all the fourteen variables identified in the preceding paragraph and V9. Then we checked all the stellar parameters of

<sup>3</sup> <http://www.aavso.org/vsx/>

Table 2: Basic Parameters of the Detected Variable stars in the field of the open cluster NGC 188

ID	Coords (J2000) (hh mm ss dd mm ss)	G (mag)	BP-RP (mag)	Distance (pc)	parallax mas	pmRA mas/yr	pmDE mas/yr	Amplitude (mag)	Period (day)	Memb (yes/no?)	$T_{eff}$ (K)	Type
V1	00 46 54.53 +85 21 44.1	16.525(6)	1.12(2)	1587 <sup>+98</sup> <sub>-87</sub>	0.58(4)	-2.47(5)	-0.84(4)	0.43(5)	0.28961(2)	yes	5423 ± 300	EW/KW
V2	00 47 33.92 +85 16 24.8	16.49(1)	1.16(6)	1568 <sup>+97</sup> <sub>-86</sub>	0.61(4)	-2.47(5)	-0.76(4)	0.83(6)	0.30675(2)	yes	5293 ± 261	EW/KW
V3	00 50 27.76 +85 15 09.1	15.66(1)	1.05(5)	1214 <sup>+43</sup> <sub>-34</sub>	0.80(3)	-0.09(4)	-1.88(3)	0.72(5)	0.28575(2)	no	5391 ± 155	EW/KW
V4	00 50 50.37 +85 16 12.9	15.688(9)	1.06(4)	2077 <sup>+87</sup> <sub>-109</sub>	0.47(3)	-2.44(3)	-0.79(3)	0.46(4)	0.34209(2)	yes	5502 ± 340	EW/KW
V5	00 46 12.12 +85 14 02.0	16.14(1)	1.10(5)	1713 <sup>+101</sup> <sub>-86</sub>	0.54(3)	-1.87(4)	-0.94(4)	0.44(9)	0.32849(4)	yes	5464 ± 270	EW/KW
V6	00 47 16.44 +85 15 35.4	15.933(3)	1.04(1)	1758 <sup>+78</sup> <sub>-88</sub>	0.54(3)	-2.24(4)	-0.98(3)	0.14(4)	0.33014(6)	yes	5447 ± 231	EW/KW
V7	00 33 48.89 +85 29 22.3	15.147(7)	1.01(3)	1105 <sup>+22</sup> <sub>-25</sub>	0.88(2)	6.05(2)	4.07(3)	0.45(4)	0.31602(2)	no	5552 ± 223	EW
V8	00 44 10.18 +84 54 13.0	17.480(8)	1.84(5)	948 <sup>+49</sup> <sub>-46</sub>	0.96(7)	-4.04(8)	-1.57(8)	0.8(1)	0.27707(4)	no	4252 ± 315	EW
V9	00 49 22.30 +84 52 57.6	16.392(7)	1.01(2)	2990 <sup>+344</sup> <sub>-286</sub>	0.31(4)	-1.38(5)	-0.61(4)	0.43(5)	0.38597(5)	yes	5578 ± 166	EW
V10	00 51 15.03 +85 24 51.1	15.512(3)	0.97(1)	1716 <sup>+92</sup> <sub>-68</sub>	0.55(2)	-2.24(3)	-0.60(3)	0.14(3)	0.35794(5)	yes	5648 ± 119	EW
V11	01 01 50.68 +85 24 00.3	13.005(4)	0.793(8)	1029 <sup>+271</sup> <sub>-202</sub>	0.6(3)	-9.4(3)	8.4(3)	0.11(4)	0.321(3)	no	–	EW
V12	00 48 22.88 +85 15 54.9	15.826(5)	1.21(2)	2054 <sup>+98</sup> <sub>-72</sub>	0.49(3)	-2.46(4)	-1.06(3)	0.31(4)	0.58426(8)	yes	5287 ± 458	EB
V13	00 52 08.76 +85 19 05.9	17.622(4)	1.34(2)	1669 <sup>+183</sup> <sub>-128</sub>	0.52(7)	-2.3(1)	-0.86(8)	0.2(1)	0.3048(3)	yes	4842 ± 358	EB
V14	01 02 23.28 +85 23 49.1	13.49(1)	0.64(5)	3705 <sup>+143</sup> <sub>-131</sub>	0.24(1)	8.21(1)	-0.95(1)	0.47(4)	0.4980(2)	no	6673 ± 228	RRAB
V15	00 34 05.31 +84 51 59.0	14.106(6)	0.72(1)	1416 <sup>+452</sup> <sub>-261</sub>	-1.2(6)	3.9(7)	2.4(8)	0.14(4)	0.23646(9)	no	–	RRC
V16	00 57 47.95 +85 02 29.0	13.540(2)	0.889(6)	773 <sup>+7</sup> <sub>-6</sub>	1.27(1)	-13.17(1)	7.97(2)	0.16(4)	0.873(2)	no	5673 ± 129	VAR
V17	00 43 23.96 +85 20 32.5	14.986(3)	0.762(7)	1863 <sup>+49</sup> <sub>-48</sub>	0.51(2)	-2.36(2)	-1.03(2)	0.05(3)	0.227(1)	yes	6246 ± 246	VAR
V18	00 48 54.43 +84 58 31.6	15.492(3)	0.803(8)	1850 <sup>+93</sup> <sub>-76</sub>	0.51(2)	5.33(3)	3.93(3)	0.09(4)	0.31698(9)	no	6116 ± 179	EW
V19	00 52 37.72 +85 10 34.6	14.599(3)	0.888(6)	1841 <sup>+84</sup> <sub>-49</sub>	0.51(2)	-2.27(2)	-0.82(2)	0.62(6)	–	yes	5888 ± 284	EA
V20	00 59 34.13 +85 03 08.4	12.802(3)	0.835(5)	635 <sup>+6</sup> <sub>-5</sub>	1.55(1)	8.11(2)	-5.79(2)	0.48(5)	–	no	5859 ± 105	EA
V21	00 44 52.20 +85 15 54.3	15.596(3)	0.969(8)	1831 <sup>+96</sup> <sub>-102</sub>	0.52(3)	-2.24(3)	-1.21(3)	0.51(6)	–	yes	5644 ± 128	EA
V22	00 32 21.20 +85 18 38.0	14.341(4)	1.36(2)	1825 <sup>+50</sup> <sub>-43</sub>	0.52(1)	-2.24(2)	-1.17(2)	0.13(3)	–	yes	4703 ± 143	L:
V23	00 39 00.88 +85 28 15.4	13.319(4)	1.33(1)	3211 <sup>+108</sup> <sub>-125</sub>	0.28(1)	-3.20(1)	1.29(1)	0.10(3)	–	no	4822 ± 231	L:
V24	00 42 40.49 +85 16 49.4	15.005(3)	1.196(9)	1821 <sup>+77</sup> <sub>-65</sub>	0.52(2)	-2.41(2)	-1.03(2)	0.10(3)	–	yes	5163 ± 316	LB
V25	00 45 23.00 +85 12 38.0	13.770(4)	1.17(2)	1906 <sup>+42</sup> <sub>-47</sub>	0.50(1)	-2.30(1)	-0.98(1)	0.23(3)	–	yes	5169 ± 296	RS:

**Notes** The classification of variable stars follows the abbreviated variable star types of VSX catalog. EW/KW indicate contact systems of W Ursae Majoris-type eclipsing variables; EB indicate  $\beta$  Lyrae-type eclipsing systems; EA indicate  $\beta$  Persei-type (Algol) eclipsing systems; RS indicate RS Canum Venaticorum-type binary systems; VAR indicate variable star of unspecified type; RRAB indicate RR Lyrae variables with asymmetric light curves, while RRC indicate RR Lyrae variables with nearly symmetric light curves; L indicate slow irregular variables, while LB indicate slow irregular variables of late spectral types. And the colons after some types indicate that the type of the variable star is not yet determined.

the fifteen stars in the other subgraphs in 5. In Figure 5 (a), most red dots are concentrated in the center of the subgraph, V22 and V9 are two slightly distant dots. Figure 5 (c) is the histogram of parallax( $\omega$ ) and Figure 5 (d) presents the observed color-magnitude diagram without reddening considered. None of the fifteen stars can be excluded as non-members. To confirm the membership of V9, we checked the catalog of Cantat-Gaudin et al. (2018), which provided the membership probabilities for 883 sources in the field of NGC 188 using UPMASK, and no records found. However, we found that Platais et al. (2003) classified V9 as a possible member star ( the probability is 73 %) using the astrometry of Tycho-2 catalog.

The absolute magnitude  $M_G$  versus intrinsic color item  $G_{BP} - G_{RP}$  CMD for the open cluster NGC 188 is shown in Figure 6. The absolute magnitude  $M_G$  is transformed by the observational magnitude  $G_{mag}$  and distance of each member star. The distances are taken from Bailer-Jones et al. (2021) estimated by probabilistic methods using a 3D a priori model of the Galaxy based on Gaia EDR3 data. We calculated the extinction coefficients  $A_G$ ,  $A_{BP}$ , and  $A_{RP}$  as follows:

$$A_M/A_V = c_{1M} + c_{2M}(G_{BP} - G_{RP}) + c_{3M}(G_{BP} - G_{RP})^2 + c_{4M}(G_{BP} - G_{RP})^3 + c_{5M}A_V + c_{6M}A_V^2 + c_{7M}(G_{BP} - G_{RP})A_V \quad (1)$$

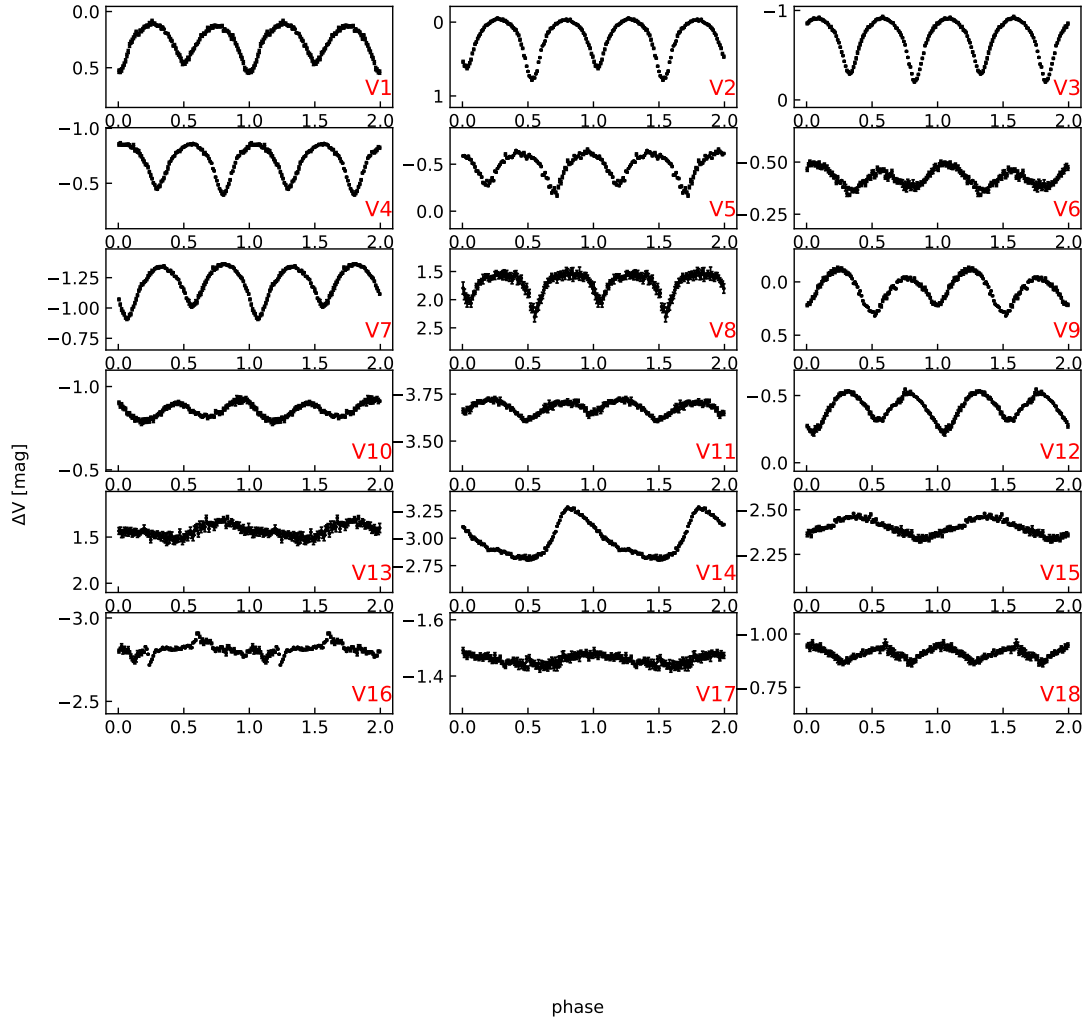


Fig. 3: The phased light curves of periodic variable stars.

This is the transformation relation for Gaia bands defined by Gaia Collaboration et al. (2018), where  $M$  represents for G, BP or RP band, and  $c_{1...7M}$  represent a set of coefficients.

The Padova theoretical isochrone (Bressan et al. 2012) is represented by a black solid line in Figure 6. For the metallicity, we adopted the metal value  $[Fe/H] = +0.064 \pm 0.018$  dex provided by WIYN/Hydra spectra of Sun et al. (2022). Other cluster parameters adopted are taken from Cantat-Gaudin et al. (2020) ( $\log(t) = 9.85$  yr,  $Z = 0.0152$ ,  $V - M_V = 11.15$  mag,  $A_V = 0.21$  mag).

## 4 RESULTS AND DISCUSSION

### 4.1 Compared to Previous Works

The four well-known W UMa variable stars identified by Hoffmeister (1964), V1 - V4, are easily detected in our observations. The suspected variable NSV 395 was not included in our field of view. All the variables identified by Kaluzny & Shara (1987) were detected in our observations, but only the light curves of three variables (V5, V6, V12), showed large enough variabilities. NSV 15158 (V25) was con-

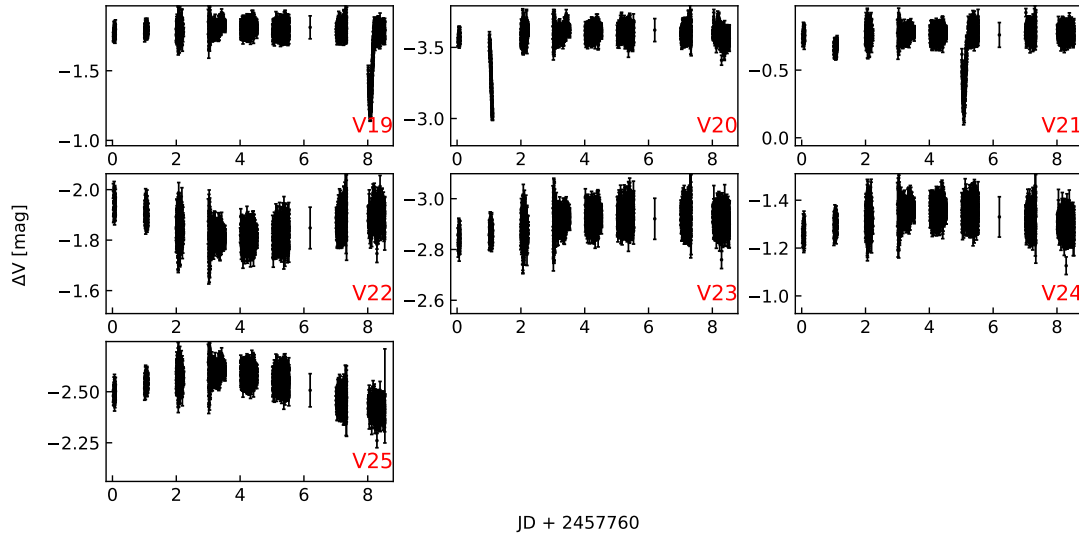


Fig. 4: The light curves of long-period variable stars.

firmed in this work. The variations of the variables discovered by Xin, Zhang, & Deng (2002) were also detected in this work, except two outside of the field of view. None of the faint variables found by Kafka & Honeycutt (2003) were confirmed in our catalog. Among the eight variables identified by Zhang et al. (2004), three of them were outside of the field of view, and no variations were found in the other three light curves, only two variables (V9, V15) were confirmed in this work. It is difficult to observe the variations of the BY Draconis type variables discovered by Mochejska et al. (2008) due to the telescope's limitation. The eclipsing binary (V13) and one BY Draconis type star (V21) of Mochejska et al. (2008) were detected in this work. Among the eighteen variables of Popov et al. (2013), eleven were out of the field of view, and the light curves of two variables were flat in our observations, the other five were confirmed in this work. The four suspected variables, are detected in our observation, while NSV 15164 is saturated, and the light curves of the other three variables did not show changes. None of the variables discovered by the TAROT Suspected Variable Star Catalog (TSVSC1) are confirmed by this work. For the two variables detected by ASAS-SN, the detached eclipsing binary (V20) was detected, but there were no variations detected in the light curve of another variable in this work. All the detected 24 known variables are listed in Table 2. Among the 24 detected known variables in the field of NGC 188, good-phased light curves were recorded for the first 17 variables listed in Table 2 as shown in Figure 3. As shown in Figure 4, the observational durations of the other seven variables are not long enough to determine the period of these variable stars. All the memberships of the detected variables are listed in Table 2. We didn't investigate the known variable stars if our data are basically consistent with the previous conclusions.

V16 and V17 were found as variable stars by Popov et al. (2013). Because of the low amplitudes of their light variations, the classifications for the two stars still remain unknown. V16 is a certain foreground field star and is a spectroscopic variable star classified by Tian et al. (2020) based on the data of LAMOST DR4. V17 is a certain blue straggler star (BSS) based on the location of the CMD, and it was classified as a single-lined BSS with rapid rotation by Geller et al. (2009).

V21 was classified as a BY Draconis type variable by Mochejska et al. (2008). It was detected by our observations because an about 0.5 mag eclipse appeared in the light curve of this star, which implies that it might be an Algol-type eclipsing binary. The location of this star in our absolute  $M_G$  versus  $G_{BP} - G_{RP}$  CMD also reinforces this view. More observations for this star are needed to determine its period and properties.



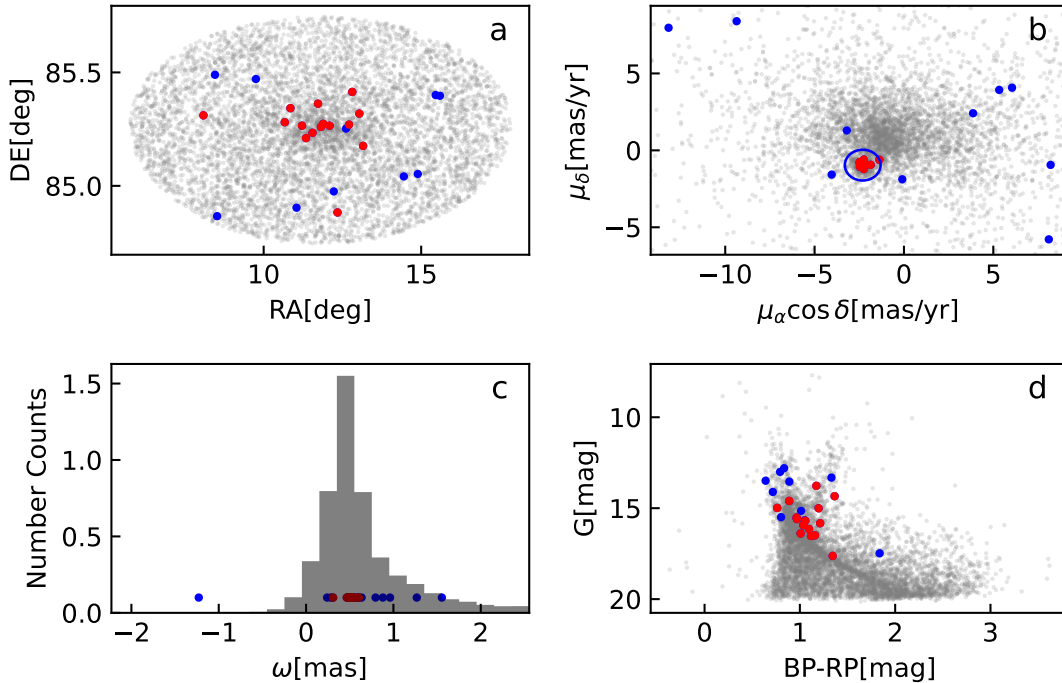


Fig. 5: (a) spatial distribution for the stars in the field of NGC 188 and 25 variable stars; (b) proper motion distribution; (c): histogram of parallax ( $\omega$ ); (d) observed color-magnitude diagram without reddening considered. In the panels, light grey dots represent the Basic Sources of Gaia DR3. Red and blue dots represent the variable members and non-members, respectively.

## 4.2 Classification of New Variables

One new periodic variable star (V18) is identified in this work. The phased light curves are shown in Figure 3, and the basic parameters for the variable are listed in Table 2. As discussed above, this is a field star with definite variations of brightness. Based on the distances of the star, V18 is a field star mixed with cluster members. We considered the period, amplitude, light-change curve shape, effective temperature, and positions on the CMD to make the classification of the variable stars obtained in this study. We checked the star's position on the CMD and compared with the statistical positions of the periodic variable stars on the CMDs given by (Gaia Collaboration et al. 2019), and found it could be a W UMa binary.

## 5 CONCLUSIONS

In this paper, we have presented the time-series V-band photometric survey of the open cluster NGC 188, with particular emphasis on variable stars. The results of this study are the following:

i). We detected 25 variable stars in a  $55 \times 45 \text{ arcmin}^2$  field of view around the cluster, including one new variable. Their memberships are determined by the research of CG20 and reconfirmed by Gaia DR3. Most results are consistent with CG20, except V9, for which is a possible cluster member in our research. Our results suggest that 15 variables are cluster members while the other 14 stars belong to the field star population.

ii). Based on the behaviors and periods of the light curves as well as their positions on the CMD, we discussed the classifications of the 25 variable stars. Most results of the known variables are coincident with the VSX catalog, except V21 (V0769 Cep), which is preferred to be an EA-type eclipsing binary

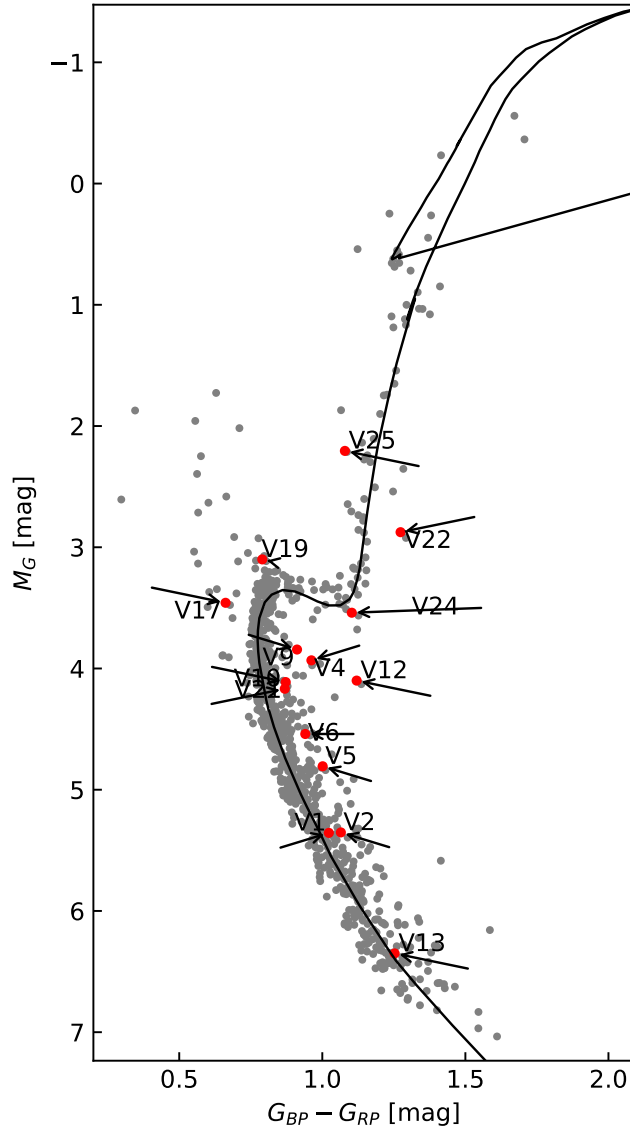


Fig. 6: CMD for cluster members of NGC 188 with the positions of the 16 cluster variables marked in red color. The cluster members are provided by CG20 with probabilities over 70 %. The cluster parameters used in the Padova theoretical isochrone fitting are come from CG20 and Sun et al. (2022).

than a BY Draconis type variable star. The new variable is likely to be a W UMa eclipsing star. The detection and analysis of the variable stars in the old open cluster NGC 188 yield valuable samples, especially for the study of W UMa stars.

**Acknowledgements** We are grateful to an anonymous referee for valuable comments which have improved the paper significantly. This work has been financially supported by the Resource sharing platform construction project of Xinjiang Uygur Autonomous Region (No. PT2306) and the Chinese Academy of Sciences (CAS) "Light of West China" Program (No. 2020-XBQNXXZ-016). This work has made use of data from the European Space Agency (ESA) mission *Gaia* (<https://>

[www.cosmos.esa.int/gaia](http://www.cosmos.esa.int/gaia)), processed by the *Gaia* Data Processing and Analysis Consortium (DPAC, <https://www.cosmos.esa.int/web/gaia/dpac/consortium>). The CCD photometric data of NGC 188 were obtained with the Nanshan 1 m telescope administered by Xinjiang Astronomical Observatory.

## References

- Anders F., Khalatyan A., Queiroz A. B. A., Chiappini C., Ardèvol J., Casamiquela L., Figueras F., et al., 2022, *A&A*, 658, A91. doi:10.1051/0004-6361/202142369
- Andrae R., Fouesneau M., Creevey O., Ordenovic C., Mary N., Burlacu A., Chaoul L., et al., 2018, *A&A*, 616, A8. doi:10.1051/0004-6361/201732516
- Bai C.-H., Feng G.-J., Zhang X., Niu H.-B., Eskandar A., Pu G.-X., Ma S.-G., et al., 2020, *RAA*, 20, 211. doi:10.1088/1674-4527/20/12/211 2
- Bai Y., Liu J., Bai Z., Wang S., Fan D., 2019, *AJ*, 158, 93. doi:10.3847/1538-3881/ab3048 5
- Bailer-Jones C. A. L., Rybizki J., Fouesneau M., Demleitner M., Andrae R., 2021, *AJ*, 161, 147. doi:10.3847/1538-3881/abd806 6
- Bertin E., Arnouts S., 1996, *A&AS*, 117, 393. doi:10.1051/aas:1996164 4
- Bonatto C., Bica E., Santos J. F. C., 2005, *A&A*, 433, 917. doi:10.1051/0004-6361:20041113 1
- Bonatto C., 2019, *MNRAS*, 483, 2758. doi:10.1093/mnras/sty3291 2
- Bressan A., Marigo P., Girardi L., Salasnich B., Dal Cero C., Rubele S., Nanni A., 2012, *MNRAS*, 427, 127. doi:10.1111/j.1365-2966.2012.21948.x 7
- Burggraaff O., Talens G. J. J., Spronck J., Lesage A.-L., Stuik R., Otten G. P. P. L., Van Eylen V., et al., 2018, *A&A*, 617, A32. doi:10.1051/0004-6361/201833142
- Cantat-Gaudin T., Jordi C., Vallenari A., Bragaglia A., Balaguer-Núñez L., Soubiran C., Bossini D., et al., 2018, *A&A*, 618, A93. doi:10.1051/0004-6361/201833476 5, 6
- Cantat-Gaudin T., Anders F., Castro-Ginard A., Jordi C., Romero-Gómez M., Soubiran C., Casamiquela L., et al., 2020, *A&A*, 640, A1. doi:10.1051/0004-6361/202038192 1, 2, 5, 7
- Carrera R., Casamiquela L., Carbajo-Hijarrubia J., Balaguer-Núñez L., Jordi C., Romero-Gómez M., Blanco-Cuaresma S., et al., 2022, *A&A*, 658, A14. doi:10.1051/0004-6361/202141832
- Clem J. L., Landolt A. U., 2016, *AJ*, 152, 91. doi:10.3847/0004-6256/152/4/91
- Cohen R. E., Geller A. M., von Hippel T., 2020, *AJ*, 159, 11. doi:10.3847/1538-3881/ab59d7 1
- Czesla S., Schröter S., Schneider C. P., Huber K. F., Pfeifer F., Andreasen D. T., Zechmeister M., 2019, *ascl.soft. ascl:1906.010 4*
- Damerdjy Y., Klotz A., Boër M., 2007, *AJ*, 133, 1470. doi:10.1086/511747
- Dias W. S., Alessi B. S., Moitinho A., Lépine J. R. D., 2002, *A&A*, 389, 871. doi:10.1051/0004-6361:20020668
- Donor J., Frinchaboy P. M., Cunha K., O'Connell J. E., Allende Prieto C., Almeida A., Anders F., et al., 2020, *AJ*, 159, 199. doi:10.3847/1538-3881/ab77bc
- Evans D. W., Riello M., De Angeli F., Carrasco J. M., Montegriffo P., Fabricius C., Jordi C., et al., 2018, *A&A*, 616, A4. doi:10.1051/0004-6361/201832756 5
- Ferraz-Mello S., 1981, *AJ*, 86, 619. doi:10.1086/112924
- Flynn C., Sekhri R., Venville T., Dixon M., Duffy A., Mould J., Taylor E. N., 2022, *MNRAS*, 509, 4276. doi:10.1093/mnras/stab3156
- Fornal B., Tucker D. L., Smith J. A., Allam S. S., Rider C. J., Sung H., 2007, *AJ*, 133, 1409. doi:10.1086/511419 1, 2
- Friel E. D., Jacobson H. R., Pilachowski C. A., 2010, *AJ*, 139, 1942. doi:10.1088/0004-6256/139/5/1942 1
- Gaia Collaboration, Prusti T., de Bruijne J. H. J., Brown A. G. A., Vallenari A., Babusiaux C., Bailer-Jones C. A. L., et al., 2016, *A&A*, 595, A1. doi:10.1051/0004-6361/201629272 1
- Gaia Collaboration, Babusiaux C., van Leeuwen F., Barstow M. A., Jordi C., Vallenari A., Bossini D., et al., 2018, *A&A*, 616, A10. doi:10.1051/0004-6361/201832843 2, 7

- Gaia Collaboration, Eyer L., Rimoldini L., Audard M., Anderson R. I., Nienartowicz K., Glass F., et al., 2019, *A&A*, 623, A110. doi:10.1051/0004-6361/201833304 9
- Gaia Collaboration, 2022, *yCat*, I/355 5
- Gaia Collaboration, 2022, *yCat*, I/358 2, 5
- Geller A. M., Mathieu R. D., Harris H. C., McClure R. D., 2008, *AJ*, 135, 2264. doi:10.1088/0004-6256/135/6/2264 2
- Geller A. M., Mathieu R. D., Harris H. C., McClure R. D., 2009, *AJ*, 137, 3743. doi:10.1088/0004-6256/137/4/3743 8
- Gillen E., Hillenbrand L. A., Stauffer J., Aigrain S., Rebull L., Cody A. M., 2020, *MNRAS*, 495, 1531. doi:10.1093/mnras/staa1016 1
- Hills S., von Hippel T., Courteau S., Geller A. M., 2015, *AJ*, 149, 94. doi:10.1088/0004-6256/149/3/94 1
- Hoffmeister C., 1964, *AN*, 288, 49. doi:10.1002/asna.19652880402 2, 7
- Huang C. X., Vanderburg A., Pál A., Sha L., Yu L., Fong W., Fausnaugh M., et al., 2020, *RNAAS*, 4, 204. doi:10.3847/2515-5172/abca2e
- Jacobson H. R., Pilachowski C. A., Friel E. D., 2011, *AJ*, 142, 59. doi:10.1088/0004-6256/142/2/59
- Kafka S., Honeycutt R. K., 2003, *AJ*, 126, 276. doi:10.1086/375649 2, 8
- Kaluzny J., Shara M. M., 1987, *ApJ*, 314, 585. doi:10.1086/165087 2, 7
- Kaluzny J., 1990, *AcA*, 40, 61 2
- Kawahara H., Masuda K., MacLeod M., Latham D. W., Bieryla A., Benomar O., 2018, *AJ*, 155, 144. doi:10.3847/1538-3881/aaaaaf
- Kazarovets E. V., Samus N. N., Durlevich O. V., 1998, *IBVS*, 4655, 1
- Kochanek C. S., Shappee B. J., Stanek K. Z., Holoién T. W.-S., Thompson T. A., Prieto J. L., Dong S., et al., 2017, *PASP*, 129, 104502. doi:10.1088/1538-3873/aa80d9
- Krone-Martins A., Moitinho A., 2014, *A&A*, 561, A57. doi:10.1051/0004-6361/201321143 5
- Li C.-Y., Esamdin A., Zhang Y., Song F.-F., Zeng X.-Y., Chen L., Niu H.-B., et al., 2021, *RAA*, 21, 068. doi:10.1088/1674-4527/21/3/068 4
- Ma S.-G., Esamdin A., Ma L., Niu H.-B., Fu J.-N., Zhang Y., Liu J.-Z., et al., 2018, *Ap&SS*, 363, 68. doi:10.1007/s10509-018-3289-y 2, 4
- Mochejska B. J., Stanek K. Z., Sasselov D. D., Szentgyorgyi A. H., Cooper R. L., Hickox R. C., Hradecky V., et al., 2008, *AcA*, 58, 263 2, 5, 8
- Monteiro H., Dias W. S., Moitinho A., Cantat-Gaudin T., Lépine J. R. D., Carraro G., Paunzen E., 2020, *MNRAS*, 499, 1874. doi:10.1093/mnras/staa2983 2
- Özeren F. F., Arslan Ö., Küçük İ., Oralhan İ. A., 2014, *NewA*, 32, 36. doi:10.1016/j.newast.2014.04.003 1
- Piskunov A. E., Kharchenko N. V., Röser S., Schilbach E., Scholz R.-D., 2006, *A&A*, 445, 545. doi:10.1051/0004-6361:20053764 1
- Platais I., Kozhurina-Platais V., Mathieu R. D., Girard T. M., van Altena W. F., 2003, *AJ*, 126, 2922. doi:10.1086/379677 6
- Popov A. A., Krushinsky V. V., Avvakumova E. A., Burdanov A. Y., Punanova A. F., Zalozhniĭ I. S., 2013, *OEJV*, 157, 1 2, 8
- Sales-Silva J. V., Daflon S., Cunha K., Souto D., Smith V. V., Chiappini C., Donor J., et al., 2022, *ApJ*, 926, 154. doi:10.3847/1538-4357/ac4254
- Sandage A., 1962, *ApJ*, 135, 333. doi:10.1086/147274
- Sarajedini A., von Hippel T., Kozhurina-Platais V., Demarque P., 1999, *AJ*, 118, 2894. doi:10.1086/301149 1
- Shan Z., Yang J., Sanjuán M. A. F., Wu C., Liu H., 2022, *EPJP*, 137, 50. doi:10.1140/epjp/s13360-021-02279-x 5
- Song F.-F., Esamdin A., Ma L., Liu J.-Z., Zhang Y., Niu H.-B., Yang T.-Z., 2016, *RAA*, 16, 154. doi:10.1088/1674-4527/16/10/154 2, 4
- Sun Q., Deliyannis C. P., Twarog B. A., Anthony-Twarog B. J., Cummings J. D., Steinhauer A., 2022, *MNRAS*, 513, 5387. doi:10.1093/mnras/stac1251 7, 10

- Tarricq Y., Soubiran C., Casamiquela L., Castro-Ginard A., Olivares J., Miret-Roig N., Galli P. A. B., 2022, *A&A*, 659, A59. doi:10.1051/0004-6361/202142186 5
- Tian Z., Liu X., Yuan H., Fang X., Chen B., Xiang M., Huang Y., et al., 2020, *ApJS*, 249, 22. doi:10.3847/1538-4365/ab9904 8
- Wang J., Ma J., Wu Z., Wang S., Zhou X., 2015, *AJ*, 150, 61. doi:10.1088/0004-6256/150/2/61 1, 2
- Xin Y., Zhang X.-B., Deng L.-C., 2002, *ChJAA*, 2, 481. doi:10.1088/1009-9271/2/6/481 2, 8
- Zacharias N., Finch C. T., Girard T. M., Henden A., Bartlett J. L., Monet D. G., Zacharias M. I., 2013, *AJ*, 145, 44. doi:10.1088/0004-6256/145/2/44 4
- Zechmeister M., Kürster M., 2009, *A&A*, 496, 577. doi:10.1051/0004-6361:200811296 4
- Zhang X. B., Deng L., Zhou X., Xin Y., 2004, *MNRAS*, 355, 1369. doi:10.1111/j.1365-2966.2004.08418.x 2, 8